COERbuoy1 - A benchmark problem for wave energy converter control strategies

Please observe

A detailed introduction in COERbuoy1 can be found in [8]. Two correction were made:

1. A torsion sping was added, see (27)
2. $\dot{x}_{w,k}$ in (10) in [8] is the speed of the body, not the relative speed between body and wave. See (5).

1 Introduction

Wave energy converter (WECs), hence machines that transforms the energy transported in ocean waves into electricity, may become a vital part in tomorrow's energy mix. A challenge is to lower the costs per power unit to become competitive with existing technologies. Energy maximizing controls are an promising way to achive this. In recent years numerous appraoches for WEC control strategy were presented for different WEC concepts. However, the strong coupling between control and WEC design prohibits a straightforward comparison of publication using different WEC designs.

WEC model The idea of the COERbuoy1 benchmark problem is to provide a WEC model that covers all significant control challenges a real WEC faces and is general enough to allow universal findings. The COERbuoy1 model simulates the following real world problems::

- Submergence dependent hydrodynamic forces
- Identification errors in the mathematical model
- Motion constraints
- Friction effects
- A non-ideal power-take-off

Benchmark tool Controller written for this model can then use the integrated benchmark process of COERbuoy1 to evaluate the controller ability to

- capture energy in narrow banded sea states
- capture energy in sea states with a wide spectrum
- deal with modeling error
- keep the stroke constraint

Table 1: Sensor data and manipulated variables

Variable	Quantity	Units
	Sensor data	
ς	Stroke length	`m`
α	Pitch angle	`rad`
$\dot{\varsigma}$	Stroke velocity	`m/s`
$\dot{\alpha}$	Pitch angular velocity	`rad/s`
F_{mo}	Force on the mooring	`N`
	Manipulated variables	
F_{gen}	Generator force	`N`
F_{br}	Braking force	`N`

COERbuoy1 is an open-source project[1] and allows the integration of controller written in every programming language using a TCP/IP based *control interface*.

2 Manipulated variables and sensor measurements

The controller receives the following data from the model: stroke position ς, the time derivation of the stroke position $\dot{\varsigma}$, the pitch angle of the WEC α and its time derivation $\dot{\alpha}$, both relative to the equilibrium position (see Figure 1), and the force along the mooring line F_{mo}. Sensor data from the model is noise-free and unbiased. Two actuators are built into the COERbuoy1 WEC: (i) The WEC can be controlled passively by setting the generator resisting force, applying a generator force opposing the direction of travel. (ii) The WEC can be controlled activley actively, by putting power into the generator at various intervals, causing a force in the direction of travel. (iii) The third option is dissipative braking, where the force is only limited by the maximal braking power P_{br}^{max}. There are no costs for applying the brake, the energy however, unlike the passive PTO-force, is not absorbed.

See Table 1 for the exchanged data.

[1] Source code available at https://github.com/SiHeTh/COERbuoyOne

3 Model

The COERbuoy1 model is a WEC of the heave-point absorber class, meaning that it generates the power mostly by the motion in heave direction. The buoy movement is restricted to the heave and surge direction. All hydrodynamic forces are calculated body-exact, meaning at the instantaneous wetted body-surface under the assumptions of linear hydrodynamics. Friction is modeled with a static (constant force at rest), a kinetic (constant force while moving) and a damping (velocity dependent force) part. Inspired by the CorPower wave energy device, a spring opposing the buoyancy stiffness is installed between translator and generator, so that the motion response in amplified (*passive control*). The stroke length is limited to ±3.5 m from the mean position. There is no fixed limit for the generator force, however, these can be obtained by the electrical limits of the generator. The COERbuoy1 WEC is anchored with a stiff line to the sea bed, where it is mounted with a pivot joint. A sketch can be seen in Figure 1. A torsion spring reduces hereby the angular movement. Buoy and the stiff line are connected with a power-take-off (PTO) mechanism.

The position vector, in global coordinates, for surge (x_1) and heave (x_3) is $\vec{x}_p = [x_1\ x_3]^T$. The global coordinates are transferred into body coordinates described in polar coordinates by the stroke length ς and the pitch angle α of the mooring line as shown in Figure 1:

$$\vec{\varsigma} = \begin{bmatrix} \varsigma \\ \alpha \end{bmatrix} = \begin{bmatrix} ||\vec{x}_p|| \\ \angle(\vec{x_p + l_m}) \end{bmatrix}. \tag{1}$$

The equation of motion is

$$\begin{aligned} \ddot{\vec{x}} =& (\vec{F}_{hy}(\vec{x}) + \vec{F}_D(\vec{x}) + \vec{F}_r(\vec{x}) + \vec{F}_b + \\ & \vec{F}_{fs} + \vec{F}_{gen} + \vec{F}_m + \vec{F}_{br} + \vec{F}_{sp} + \vec{F}_g)/(m + \vec{m}_a) \end{aligned} \tag{2}$$

where m is the mass, m_a the hydrodynamic high frequency limit of the added mass, $\vec{F}_{hy}$ the excitation force, $\vec{F}_D$ the viscous drag force, $\vec{F}_r$ the radiated wave force, $\vec{F}_b$ the buoyancy force, $\vec{F}_{fs}$ the force from the buoyancy opposing spring, $\vec{F}_m$ the machinery friction force, $\vec{F}_{sp}$ the force of the torsion spring and $\vec{F}_g = mg$ the gravity force, with $g = 9.82\frac{m}{s^2}$ the gravitational acceleration. The generator force $\vec{F}_{gen}$ and the friction brake force $\vec{F}_{br}$ can be set arbitrarily (within limits). The remainder of this Section describes the body-exact hydrodynamic force (Subsection 3.1) and the machinery forces in Subsection 3.2.

3.1 Hydrodynamic forces

Linear hydrodynamics allows to describe ocean wave as a sum of sinusoidal waves with different wave frequencies, thus

$$\begin{aligned} \hat{\boldsymbol{\eta}}(\omega) &= \mathcal{F}(\eta(t)) \\ \hat{\boldsymbol{\eta}}_{tx}(\omega) &= |\hat{\boldsymbol{\eta}}(\omega)| \cos(\omega t_x + \angle\hat{\boldsymbol{\eta}}(\omega)) \\ \eta(t_x) &= \Re\left(\int_\omega \hat{\boldsymbol{\eta}}(\omega, t_x) d\omega\right), \end{aligned} \tag{3}$$

with $\hat{\boldsymbol{\eta}}$ being the (complex) frequency spectrum of the wave. $\hat{\boldsymbol{\eta}}_{tx}$ is the instantaneous wave spectrum at time t_x and $\eta(t_x)$ the instantaneous wave height.

Furthermore linear hydrodynamics allows to split the hydrodynamic forces into three components: (1) the undisturbed incoming wave, (2) the scattered wave field by the non-moving buoy, and (3) the radiated wave caused by the buoy's movement [3]. The undisturbed incoming and the scattered wave act on the not moving body and result in the excitation force:

$$F_{hy,j}(t) = \hat{\boldsymbol{h}}_{ex,j}(x(t), z(t))\hat{\boldsymbol{\eta}}, \tag{4}$$

with $\hat{\boldsymbol{h}}_{ex}$ being the complex spectral excitation force coefficients, evaluated at the instantaneous body position $(x(z), z(t))$ and j being the direction. The radiated wave is calculated similarly

$$F_{r,j}(t_x) = \int_0^{t_x} \left(\int_\omega c_h \boldsymbol{h}_{r,j}(\tau)\cos(\omega(t_x - \tau))d\omega\right) \dot{x}_j(\tau)\delta(\tau)d\tau\ , \tag{5}$$

with c_h a coefficients transforming $|\hat{\boldsymbol{h}}_{ex,j}|^2$ into the radiation resistance in spectral domain $\boldsymbol{h}_{r,j}$ (Haskind relation):

$$c_h = 2\pi(\omega k)/(4\pi g^2 \rho). \tag{6}$$

Furthermore, $\dot{x}_j$ is the buoy's velocity in degree of freedom j and δ is the Dirac impulse.

The buoyancy force is obtained by integrating the static pressure over the wetted surface of the buoy, as described in [5].

Viscous drag The viscous drag in heave and surge is calculated based on the actual projected wetted surface $S_{w,j}$ and a drag coefficients $c_{D,j}$:

$$F_{D,j} = S_{w,j} c_{D,j} \dot{x}_j |\dot{x}_j|. \tag{7}$$

3.2 Machinery forces

Stribeck friction The machinery losses are simulated as a Stribeck friction curve, with static friction $F_{fr,s}$, dynamic friction $F_{fr,k}$, and a friction damping term γ_f:

$$\ddot{\varsigma} = 0 \qquad \text{, if } \dot{\varsigma} = 0 \wedge |M\ddot{x}\vec{n}_\varsigma| <= F_{fr,s} \tag{8}$$

$$F_m = F_{fr,k} + \gamma_f \dot{\varsigma}, \text{ otherwise,} \tag{9}$$

with $M = m + m_a$.

PTO The PTO uses a rotational direct-driven generator. A gearbox the translatory stroke speed $\dot{\varsigma}$ into the angular generator speed ω_g. The reactive power flow is assumed to set to zero ($I_d = 0$) by the generator's internal controller. By this the generator becomes:

$$p = 0.5E^2/(F_{pto}\dot{\varsigma}) \tag{10}$$

$$q = X^2 \tag{11}$$

$$E = c_\lambda \dot{\varsigma} \tag{12}$$

$$X = c_L \dot{\varsigma} \tag{13}$$

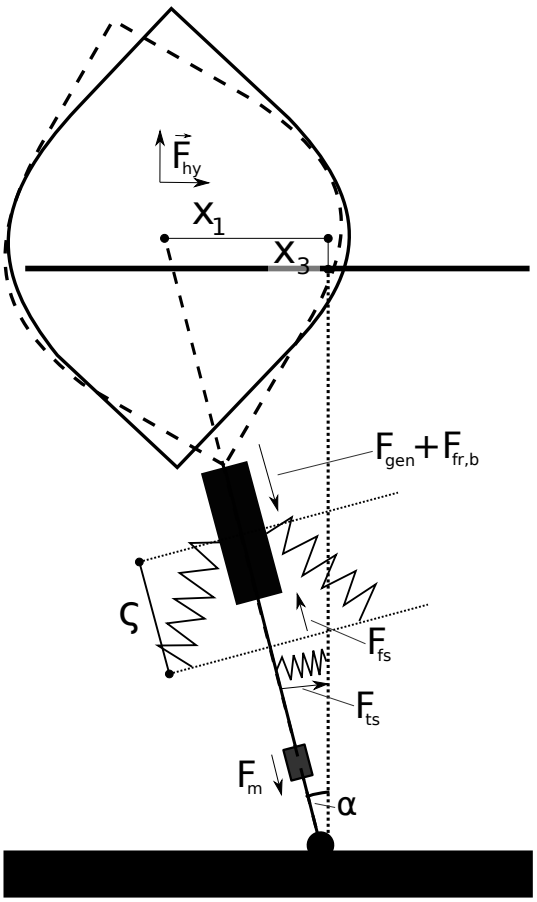

Figure 1: Schematic of the COERbuoy1 model.

Then resolve for R:

$$R^2 = pR - q \tag{14}$$

In generator mode the minium damping is limited by the internal resistance:

$$R = \max(R_c, R), \text{ if } F_{pto}\dot{\varsigma} > 0 \wedge R > 0 \tag{15}$$

The actual load is then $R_l = R - R_c E/|E|$. The actual current is then calculated in relation to the current saturation limit:

$$I_1 = E/\sqrt{R^2 + X^2} \tag{16}$$

$$\gamma = |I_s/I_1| \tag{17}$$

$$D = \begin{cases} 2/\pi(\arctan(\gamma/\sqrt{1-\gamma}) + \gamma\sqrt{1-\gamma^2}) & \text{, if } \gamma < 1 \\ 1 & \text{, else} \end{cases} \tag{18}$$

$$X = (c_L(1 + (1 - D)))\dot{\varsigma} \tag{19}$$

$$I = E/\sqrt{R^2 + X^2} \tag{20}$$

$$\tag{21}$$

Finally the appplied generator force F_{gen} and the absorbed electrical power P_{abs} are:

$$F_{gen} = E^2 R/(R^2 + X^2)/\dot{\varsigma} \tag{22}$$

$$P_{abs} = R_l I^2; \tag{23}$$

Table 2: List of COERbuoy1 parameters. [a]The mass is denoted relative to the buoyancy force at equilibrium position. The remaining buoyancy force is the pre-tension of the mooring.

Name	Symbol	Value	Range
Negative spring			
force	c_{fs}	450 kN	±0.2
length	c_{ls}	2.0 m	
stroke	s_{fs}	5 m	
Viscous drag			
heave coefficent	D_h	0.2	
surge coefficent	D_s	0.5	
Friction			
static friction	fr_s	30 kN	±0.2
kinetic friction	fr_d	15 kN	
friction damping	d_{add}	7.5 kNs/m	±0.4
Friction break			
max. power	P_{br}^{max}	1 kW	
Generator			
copper resistance	R_c	2Ω	
inductance coef.	c_L	120	
flux coef.	c_λ	8000	
saturation current	I_s	300 A	
Pitch spring			
stiffness	c_p	$10\frac{\text{N}}{\text{rad}}$	
damping	d_p	$5\frac{\text{Ns}}{\text{rad}}$	
Miscellaneous			
mooring length	l	40 m	±0.2
mass floater[a]	m_b	80 %	
stroke limit	ς_{lim}	±3.5 m	

This method was evaluated with a full-scale wave energy generator in [6].

When exceeding the stroke limits $\pm\varsigma_{lim}$, the generated power cannot be utilised and is therefore not considered in the calculated overall energy output; reactive power put into the generator, however, is always subtracted from the total absorbed energy.

Pre-tension The pre-tension force $\vec{F}_t$ allows the buoy's gravity force, and therefore its mass, to be lower than the buoyancy force at the equilibrium position, and is calculated as the mismatch between the gravity and buoyancy forces at the equilibrium position:

$$F_{t,j} = V_0 \rho g (1 - c_{m,f}), \tag{24}$$

where V_0 is the submerged volume at the equilibrium position, and $c_{m,f} \epsilon (0, 1]$ is the ratio $m/(V_0\rho)$.

Negative spring A spring contradicting the buoyancy stiffness is installed between body and the anchored line. In mean position the spring, which has a constant force is compressed and all forces acts in horizontally, thus no force actually acts in between line and body. When the body is deflected,

$$\begin{aligned} l &= \min(\max(-s_{fs}, z), s_{fs}) \\ F_{fs} &= c_{fs} \arctan(l/l_{fs}), \end{aligned} \tag{25}$$

with s_{fs} the maximal spring length. l_{fs} spring length at mean position and c_{fs} the spring force at mean position.

Braking force The braking force F_{br} opposes the direction of travel and can be set to an arbitrary value within the power limit P_{br}^{max}:

$$F_{br}\dot{\varsigma} < P_{br}^{max}. \tag{26}$$

Torsion spring To limit the pitch motion a torsion spring is installed in the mooring joint, that pushes the mooring line back in equilibrium position:

$$F_{sp} = c_p\alpha - d_p\dot{\alpha}, \tag{27}$$

with c_p being the stiffness and d_p the spring damping.

4 Benchmarking

The benchmark process consists of a total of 24 test run in three stages. Each test run is evaluated in respect of the absorbed power, and how well the constraints are kept. The sum of all test combined gives the total score.

4.1 Benchmark stages

The benchmark process consists of three stages, ranging from regular waves and an ideal model to irregular wave with model uncertainties.

(I) The first stage comprises four regular (monochromatic) waves, and uses an ideal model (all parameters as defined in this document)

(II) Stage two uses four Bretschneider waves, thus tests the controller's ability to capture power from wide-band spectra, but still uses an ideal model

(III) The third stage uses the irregular sea states from (II), but alters the parametrisation of the model. Each sea state is executed four times, but with a different set of parameters for the COERbuoy1 model.

Waves To increase readability, the regular waves are shortened to the form (T_w, H_{RMS}), where the first value indicates the wave period (T_w) in seconds and the second number corresponds to the root-mean square wave height (H_{RMS}) in meters. Similarly, the irregular sea states are shortened to the form $\{T_e, H_s\}$, where the first number corresponds to the energy period (T_e) in seconds, and the second number indicates the significant wave height (H_s) in meters. The four regular sea states are (6,1), (9,1), (9,3), (12,3), the irregular sea states are {6, 1}, {9, 1.5}, {9, 3} and {12, 3}.

Table 3: Table of sea states used in the benchmark

H_{rms}/H_s [m]	T_w/T_e [s]	$P_{ccc}[kW]$
1	6	102.6
1.5	9	426.9
3	9	938
3	12	826.3

H_{rms} and T_p apply for a regular wave, and H_s and T_e apply for an irregular sea state.

Systematic modeling error test Using alternating model parameters tests, depending on the controller design, either the controller's ability to adapt to a systematic bias or its robustness to modeling errors.

4.2 Scoring

The controller is assessed by its generated electric energy and how well it adheres to the constraints, resulting in a power score S_p and a constraint score S_c which, multiplied, give the benchmark score S_S.

Power score The absorbed power is set into relation to that absorbed by a stroke constrained complex-conjugate controller P_{ccc}, for an ideal, linear, heave only model:

$$P_{ccc} = \begin{cases} \hat{F}_e(T_w)^2/(8R(T_w)) & \text{, if } \max(\varsigma) < \varsigma_{lim} \\ 0.5u^2(\hat{F}_e(T_w)/u - R(T_w)) & \text{, otherwise} \end{cases}, \tag{28}$$

with $u = \varsigma_{lim}2\pi/T_w$ and $\hat{F}_e = 0.5H_{rms}\sqrt{2}h(T_w)$. The power score is then:

$$S_p = \max(P_{gen}/P_{ccc}, 0). \tag{29}$$

Constraint score To evaluate the controller's ability to handle the stroke limit, a) no power is absorbed when out of the allowed stroke length, b) a constraint score S_c calculated as the duration above the limit, divided by the total duration of sea state t_d:

$$S_c = t_c/t_d. \tag{30}$$

Total score The sum $S_{s,ss,sg}$ for each sea state ss at stage sg is the product of the power score $S_{p,ss,sg}$ and the constraint score $S_{c,ss,sg}$:

$$S_{s,ss,sg} = S_{p,ss,sg}S_{c,ss,sg} \tag{31}$$

The score for each stage is the mean of all sea state scores:

$$S_{s,sg} = \sum_{ss=1}^{4} S_{s,ss,sg}. \tag{32}$$

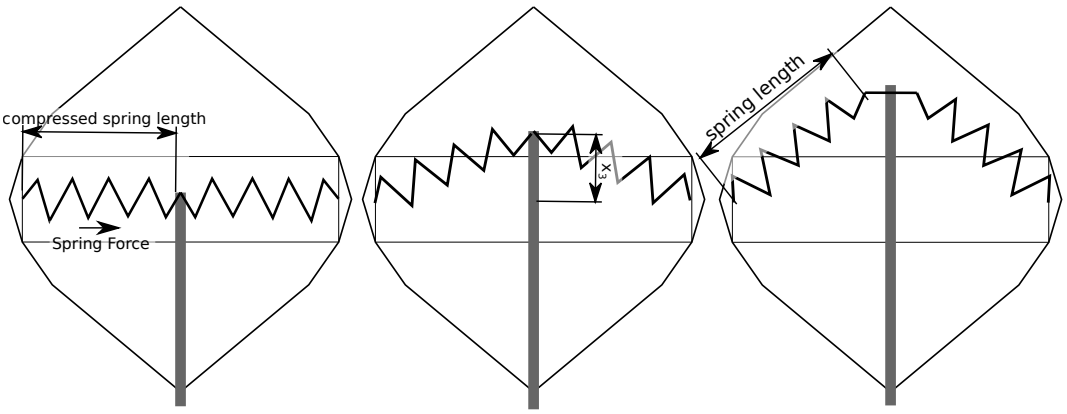

Figure 2: Sketch of the negative spring.

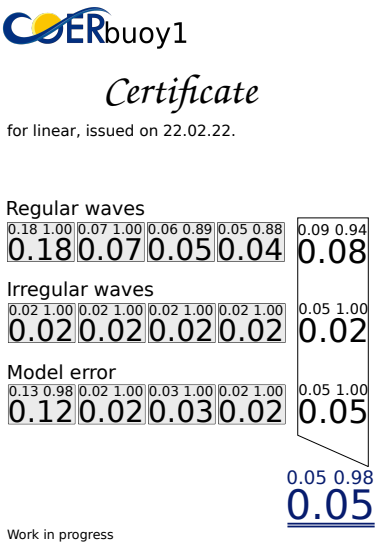

Figure 3: Draft of the benchmark certificate.

Subsequently, the final score is the mean of the scores for all stages:

$$S_{s,sg} = \sum_{sg=1}^{3} S_{s,sg}. \tag{33}$$

The software will generate a certificate showing all relevant information on one page, see Figure 3.

Acknowledgements

The authors would like to thank Giuseppe Giorgi from Politecnico di Torino, for his help in understanding hydrodynamics, Hafiz Ahsan Said, for his help with the generator model, and Carrie Anne Barry, both from COER. This research was part-funded by Science Foundation Ireland (SFI) through MaREI, the SFI Research Centre for Energy, Climate, and Marine [Grant No: 12/RC/2302_P2], with supporting funding obtained from CorPower Ocean AB.

References

[1] Nicolás Faedo, Demián García Violini, Yerai Peña Sanchez, and John Ringwood. Optimisation-vs. non-optimisation-based energy-maximising control for wave energy converters: A case study. 05 2020.

[2] Nicolás Faedo, Sébastien Olaya, and John V. Ringwood. Optimal control, mpc and mpc-like algorithms for wave energy systems: An overview. *IFAC Journal of Systems and Control*, 1:37–56, 2017.

[3] Johannes Falnes. *Ocean Waves and Oscillating Systems: Linear Interactions Including Wave-Energy Extraction*. Cambridge University Press, Cambridge, 2002.

[4] Demián García Violini, Nicolás Faedo, Fernando Jaramillo-Lopez, and John Ringwood. Simple controllers for wave energy devices compared. *Journal of Marine Science and Engineering*, 8:793, 10 2020.

[5] Giuseppe Giorgi and John V. Ringwood. Analytical representation of nonlinear froude-krylov forces for 3-dof point absorbing wave energy devices. *Ocean Engineering*, 164:749 – 759, 2018.

[6] Remya Krishna, Olle Svensson, Magnus Rahm, Sasi K. Kottayil, Rafeal Waters, and Mats Leijon. Analysis of linear wave power generator model with real sea experimental results. *IET Renewable Power Generation*, 7(5):574–581, 2013.

[7] John Ringwood, Francesco Ferri, Kelley M. Ruehl, Yi-Hsiang Yu, Ryan G. Coe, Giorgio Bacelli, Jochem Weber, and Morten Kramer. A competition for wec control systems. In *12th European Wave and Tidal Energy Conference, Cork, Ireland*, 2017.

[8] Simon Thomas, Jørgen Todalshaug, and John Ringwood. A realistic nonlinear benchmark problem for wave energy controllers - coerbuoy1. In *14th European Wave and Tidal Energy Conference*, 09 2021.

[9] Jørgen Todalshaug, Johannes Falnes, and Torgeir Moan. A comparison of selected strategies for adaptive control of wave energy converters. *Journal of Offshore Mechanics and Arctic Engineering*, 133, 03 2011.